Description of a single modular optical setup for ellipsometry, surface plasmons, waveguide modes, and their corresponding imaging techniques including Brewster angle microscopy

M. Harke, R. Teppner, O. Schulz, and H. Motschmann[a)]
Max-Planck Institut of Colloids and Interfaces, Rudower Chaussee 5, D-12489 Berlin, Germany

H. Orendi
Universität Potsdam, Institute of Solid State Physics, Kantstr. 55, D-14513 Teltow, Germany

(Received 17 March 1997; accepted for publication 9 May 1997)

A versatile modular setup is described which incorporates ellipsometry, surface plasmon spectroscopy, waveguide modes, their corresponding imaging techniques and Brewster angle microscopy in a single instrument. The important design criteria are discussed with special emphasis given to the requirements imposed by imaging under an oblique angle of incidence. Several experimental examples demonstrate the power of the instrument. Imaging nullellipsometry of a patterned monolayer on a highly reflecting support demonstrates a lateral resolution of approximately 1 μm and an accuracy in the thickness determination in the sub-nm region. The localization of the evanescent field of a surface plasmon was exploited to characterize adsorption layers in turbid and thus highly scattering solutions. An example of how an anisotropic sample can be characterized with the aid of waveguide modes is provided. © *1997 American Institute of Physics.* [S0034-6748(97)03508-9]

I. INTRODUCTION

Ellipsometry, surface plasmon spectroscopy, and waveguide modes are well established techniques for the characterization of thin films and surfaces.[1–3] These techniques allow a determination of optical constants and thicknesses of a layer system. In favorable cases the thickness can be determined to within sub-nm accuracy. Despite the apparent similarities between these techniques as far as the parameters measured are concerned, individual features of each technique can be exploited for a given experimental task. Due to each method requiring similar optical components, a versatile single modular setup can be designed at moderate cost which includes even the corresponding imaging techniques.

Ellipsometry uses the fact that the state of polarization of an incident beam changes upon reflection at a film covered surface. The change in the state of polarization can be described by two measurable quantities, Ψ and Δ, which in turn are related to the optical properties of the film.[1] An ellipsometer therefore uses polarization optics to produce and analyze any desired state of polarization. Various designs of ellipsometers are suggested in the literature differing mainly in the data accumulation procedure and the subsequent analysis algorithm.[4] A common implementation of this technique is nullellipsometry which is capable of determining the ellipsometric angles with high accuracy.[5] A distinct state of polarization of the incident beam leads to the production of linearly polarized light upon reflection. The null position of the polarization optics, which leads to a complete cancellation of the reflected beam, provides the unknown parameters Ψ and Δ. A measurement scheme based on four-zone averaging, eliminates most intrinsic imperfections in the optical components as well as many errors due to misalignment of the ellipsometer. In the case of a weakly reflecting support or measurements close to the Brewster angle, it is favorable to use an algorithm which utilizes rotating elements in the instrument. Here the intensity at the detector is recorded as a function of the setting of the analyzer or polarizer. A Fourier analysis or fitting procedure of the recorded intensity versus setting of polarizer and analyzer yields the unknown quantities. In order to optimize the accuracy in the determination of the ellipsometric angles it is required to use a predetermined optimized setting of the polarization optics for a given sample. An alternative approach using different instrumentation but the same physical concept is that of a polarization modulated ellipsometer.[6]

Surface plasmon spectroscopy and waveguide modes use evanescent waves to probe thin films.[7] A surface plasmon can be regarded as a bound electromagnetic wave propagating at the metal-dielectric interface.[2] Within a plane parallel to the interface the surface plasmon has similar properties to a free electromagnetic wave, for instance it can be diffracted. However, the electric field decays exponentially normal to the plane. The localization of the electric field provides a high surface sensitivity to changes in its vicinity. Unfortunately only a couple of metals give rise to sharp surface plasmon resonances which limits its application. In order to excite both waveguide modes and surface plasmons the sample geometry has to meet certain criteria. The projection k_x of the wave vector $\mathbf{k}$ of the incident light has to match with the corresponding quantity of the plasmon or the waveguide mode. This can be achieved with the aid of a prism coupler in the Kretschman configuration[8] or by use of a grating coupler.[9] However, surface plasmons can only be excited by using $\hat{p}$-polarized light, whereas in waveguides it is possible to guide light of different polarizations. TE modes are only governed by the thickness and the refractive index,

a)Author to whom correspondence should be addressed; Electronic mail: motschma@mpikg.fta-berlin.de

 © 1997 American Institute of Physics

n_y, pointing in the direction of the electric field vector, whereas TM modes are governed by the refractive indices n_x, n_z, and the thickness t. Waveguide modes can be successfully employed for determining the properties of anisotropic media without any ambiguity in the interpretation of the data. Waveguide mode resonances can be very sharp with a half-width of a couple of hundredths of a degree. The goniometer of the instrument must provide this accuracy.

Some surfaces under investigation are inhomogeneous on a micrometer scale due to variations in the thickness, different surface composition changes in the orientational order of the molecules at the interface. In this case the lateral inhomogeneity is imparted to the properties of the reflected light. The most well-known imaging technique for visualizing this is Brewster angle microscopy (BAM),[10,11] which has been successfully employed for characterizing the phase diagrams and the morphology of Langmuir films. BAM is based on the principle that the reflectivity of the p-polarized light is zero at the Brewster angle. Any modification of the Brewster conditions, as for instance the presence of a single monolayer, modifies the reflectivity. Visualization of the inhomogeneities requires a microscope objective and a charge-coupled device (CCD) camera. A decisive advantage of this method is that fluorescent labeling is not required, as is the case in fluorescent microscopy, and that internal structures of domains can also be assessed.[12] Ellipsometry can also be extended to an imaging technique which offer a wider field of applications.[13] In contrast to BAM, imaging is not bound to the existence of a Brewster angle and can even be employed for the investigation of monolayers on highly reflecting supports. Any inhomogeneity in the sample is transferred as an inhomogeneity of the state of polarization of the reflected beam, leading to a dark-bright pattern at the CCD camera.

Also waveguide modes or surface plasmons can be used for the visualization of inhomogeneities using similar instrumentation. An example was provided in Ref. 14, where the efficiency of the poling process of a waveguide for electro-optical applications was assessed.

All the above mentioned imaging techniques work under an oblique angle of incidence. As a result some peculiarities exist which have to be taken into account in the design of the instrument. The present contribution discusses the most relevant design features.

II. EXPERIMENTAL SETUP

Figure 1 illustrates the optical layout. Laser light can be converted to any desired state of polarization by means of a polarizer and a quarter-wave plate. The light reflected from the sample can be subsequently analyzed by means of an analyzer and a photodetector. For the imaging techniques a suitable microscope objective, a projective lens, and a CCD camera are also required. For ease of operation interchangeability of both modules should involve only a couple of steps. The angle of incidence should be controlled to within a high accuracy to meet the demands required by waveguide modes.

Figure 2 shows a photograph of our system. The heart of the instrument is a specially designed two-circle goniometer

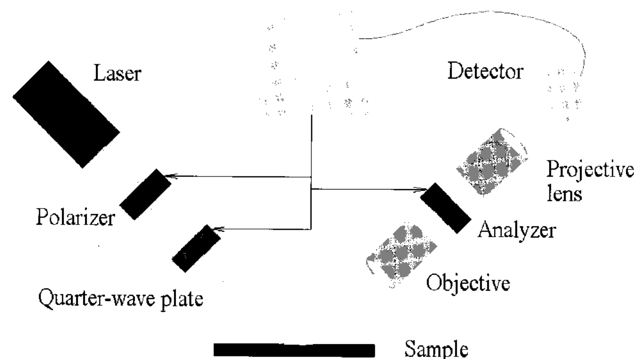

FIG. 1. Optical layout of the system, polarizer, and quarter-wave plate are used to produce any desired state of polarization of the incident beam. The reflected beam can be subsequently analyzed by means of an analyzer. Polarizer and analyzer are mounted on high precision computer controlled rotary stages. All Imaging techniques require a suitable microscope objective, a projective lens, and a CCD camera. Waveguide modes require accurate setting of the angle of incidence to within 1/1000 of a degree.

driven by dc motors and optical decoders which allow a reproducible setting of laser and detector arm to within 1/1000 of a degree. The goniometer can be manually tilted and fixed in any desired position. This design provides an optimal flexibility, e.g., some measurements require a vertical arrangement (liquids), whereas others require a tilted one (transfer of LB films). The design thus allows measurements in unusual geometries, for example the instrument is currently used for the characterization of an adsorption layer on a pendent drop in our laboratory.

The laser arm is equipped with a 40 mW intracavity frequency doubled cw Nd:YAG laser (Uniphase, FRG). The laser emits a TM_{00} mode profile providing a homogeneous illumination of the sample which is crucial for the image quality. The high intensity of the laser is desirable to compensate the tradeoff between magnification and contrast in

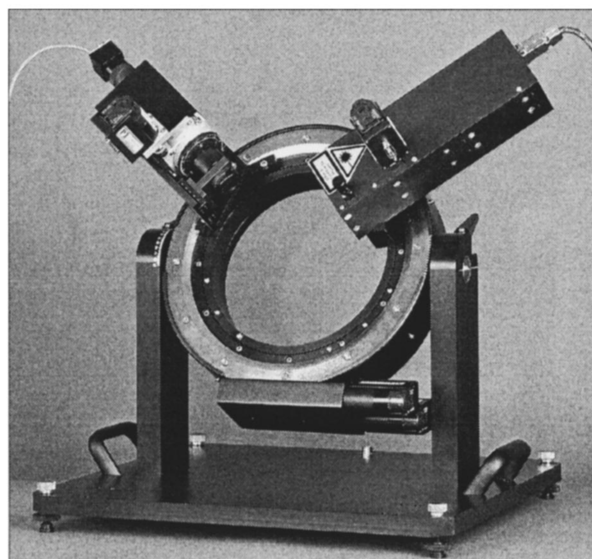

FIG. 2. Photograph of the system. Laser and detector arm are mounted on a specially designed high precision two-circle goniometer. The goniometer can be tilted and fixed in any desired position to provide flexibility for different experimental tasks.

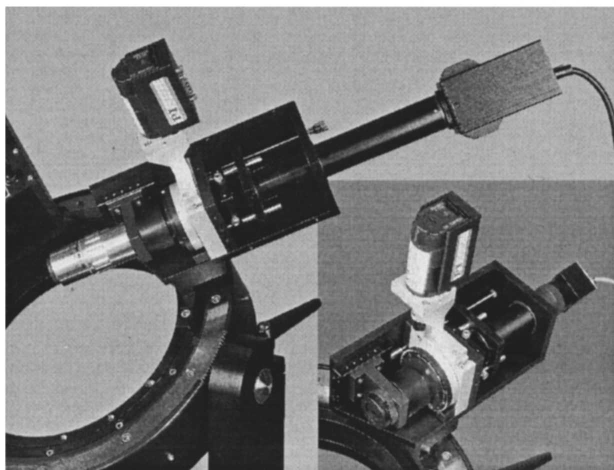

FIG. 3. Photograph of the detector arm: for imaging the iris aperture has to be replaced by an ultralong distance objective and the photodiode with the CCD camera module which contains suitable projective lenses. The focus is achieved via a translation stage which can be used for scanning to overcome the depth of field problem.

BAM or ellipsometric images. A beam of sufficient quality can also be obtained with the aid of a single mode fiber and a gas laser which are available in most optical laboratories. The optical components of the laser arm produce any desired state of polarization. The key elements are a Glan–Thompson polarizer with an extinction ratio of 10^{-8} (Halle, FRG) and a low-order retardation plate coated with an antireflection layer (Halle, FRG). Both elements are mounted on high precision rotary stages (PI, FRG). The polarizer setting can be controlled by means of a computer to within 1/1000 of a degree. This accuracy is even preserved at a rotation speed of 160°/s. The quarter-wave plate can be manually aligned to within 1/100 of a degree. Similar components are used in the detector arm. A four-quadrant diode is used as a photodetector. Alignment of the sample is achieved if the recorded intensity of all segments matches. The data are processed with the aid of an analog to digital (A/D) converter and computer. Various algorithms are implemented (e.g., null, rotating polarizer, and analyzer).

The detector arm is designed in such a way that only a couple of steps are involved in modifying it for imaging: the iris aperture is replaced by a microscope objective and the photodiode tube is replaced by the corresponding CCD module, cf. Fig. 3. The aperture of the analyzer should not limit the image formed by the objective. The lateral resolution achieved in the image is inversely proportional to the numerical aperture, A, and proportional to the wavelength, λ. Imaging under an oblique angle of incidence imposes restrictions on the ratio of diameter and working distance W of the objective. The relation between working distance W, angle of incidence α, and numerical aperture $A=n\ \sin\ \gamma/2$ is illustrated in Fig. 4: Obviously there are two limiting cases, the beam should not be chopped off by the objective and the objective should not touch the sample. The latter can be neglected if only the edge of the sample is investigated:

$$\frac{d}{2W}<\tan(2\alpha)\quad \text{and}\quad \frac{2W}{d}>\tan\ \alpha. \tag{1}$$

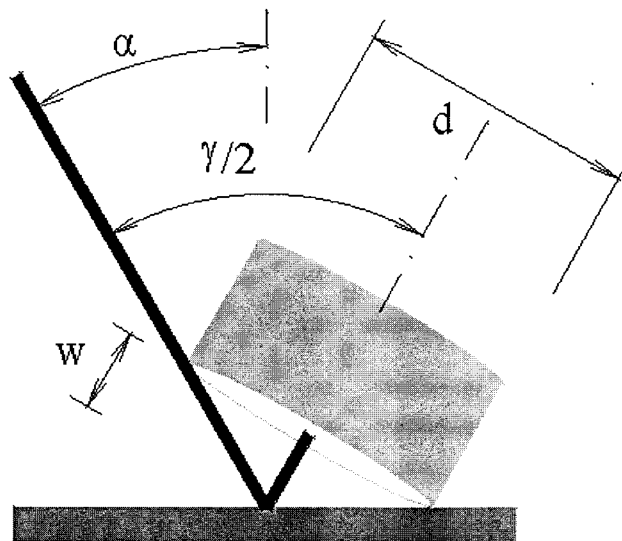

FIG. 4. Limitations imposed on the objective due to the peculiarities which arise from Imaging under an oblique angle of incidence. Abbreviations used: Working distance W, Numerical aperture $A=n\ \sin\ \gamma/2$, angle of incidence α.

The resolution, which can be achieved is given by[15]

$$b=1.22\frac{\lambda}{A}\quad \text{with}\quad A=n\ \sin\ \gamma/2, \tag{2}$$

i.e., imaging at 53° limits the numerical aperture to 0.6, which produces a maximum resolution of $\sim 1\ \mu$m at 532 nm. Figure 5(a) provides a nullellipsometric image of a self-assembled monolayer of (dimethylchlorosilyl)-2-(p,m-chloromethylphenyl)ethan on silicon. The monolayer was

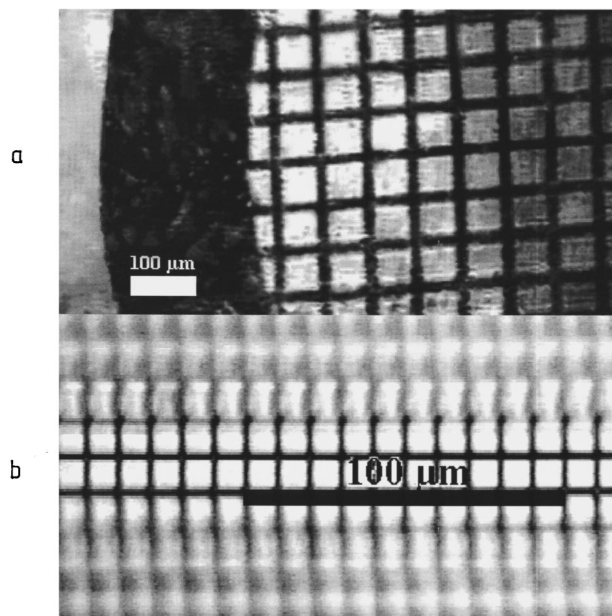

FIG. 5. (a) Nullellipsometric image of a self-assembled monolayer on a silicon wafer. The monolayer was patterned with the aid of a mask and UV light. The difference in the thickness between the dark and bright regions is 0.8 nm. (b) At high magnification problems arise due to the limited depth of field. The width of the bars are 1.9 μm, the mesh size is 10 μm, and imaging is performed at an angle of 53°.

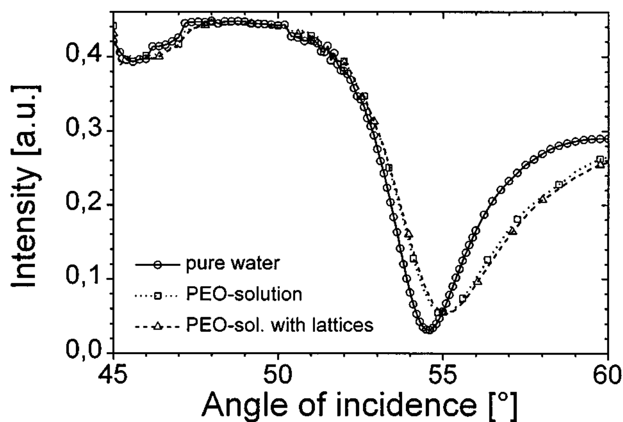

FIG. 6. *In situ* investigations of the adsorption of a water soluble polymer onto silver by surface plasmon. (a) Circle: silver–water interface before adsorption, (b) square: after adsorption of PEO, (c) triangle: after addition of lattices to the latter.

photochemically patterned using UV irradiation and an electron microscopy grid as a mask. The difference in the thickness between dark and bright parts is 0.8 nm demonstrating the high vertical resolution of this technique. At a higher magnification there are certain problems arising from the limitation of the depth of field. The depth of field, t, of an objective is given by the numerical aperture A, the refractive index n of the ambient medium, and the wavelength λ according to:[15]

$$t=\frac{n\lambda}{A^2}. \quad (3)$$

Depending on the angle of incidence, α, and the numerical aperture, A, only a region s of the illuminated part of the sample is in focus. This region, s, is of the order of 1–50 μm:

$$s=\frac{t}{\sin\alpha}. \quad (4)$$

This problem is illustrated in Fig. 5(b). The size of a bar is 1.9 μm, the mesh size is 10 μm, and imaging was performed at 53°. By scanning the surface with the objective in conjunction with imaging processing software a sharp image of the whole sample can be produced. In addition an image distortion arises due to the oblique angle of incidence. This can be compensated for by tilting of the CCD chip by α degrees with respect to the relected beam. The same can be achieved with the aid of imaging processing software. In Ref. 16 it was shown that imaging nullellipsometry can be performed using any reflecting support, e.g., for the liquid–liquid, liquid–solid, liquid–gas, solid–gas interface.

Figure 6 shows a surface plasmon scan. In this case the adsorption of a water soluble polymer [polyethyleneoxide (PEO)] on silver was studied *in situ*. The solid line (circles) refers to the plasmon resonance of the bare silver–water interface before adsorption. With the aid of a flow cuvette the water was replaced by a aqueous PEO solution. PEO adsorbs at the interface forming a thin layer of the order of 5 nm leading to a shift in the resonance (squares). Since the electromagnetic field of the surface plasmon is highly localized at the metal-dielectric interface it is only sensitive to the interfacial region and not to changes in bulk properties. To illustrate this, lattice spheres of 1 μm were added to the PEO solution thus producing a highly turbid sample. Even though the solution appeared milky white the surface plasmon resonance still matches all original features (triangles). For the sake of clarity the number of experimental points shown in Fig. 6 is reduced.

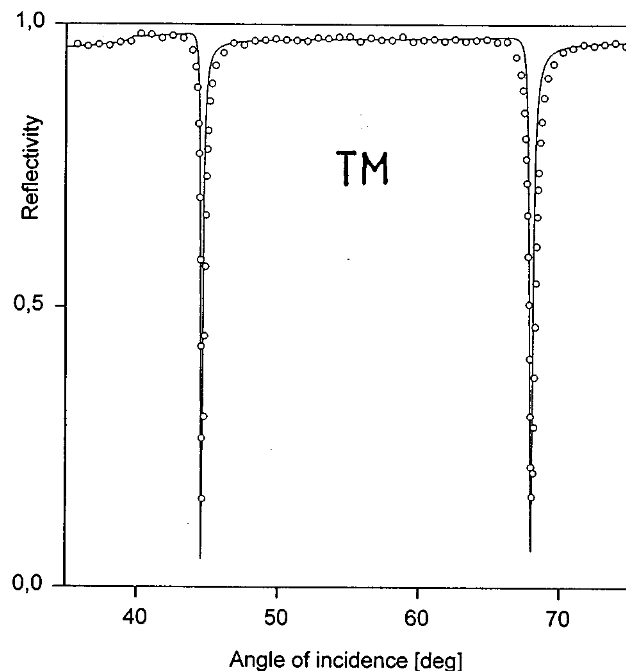

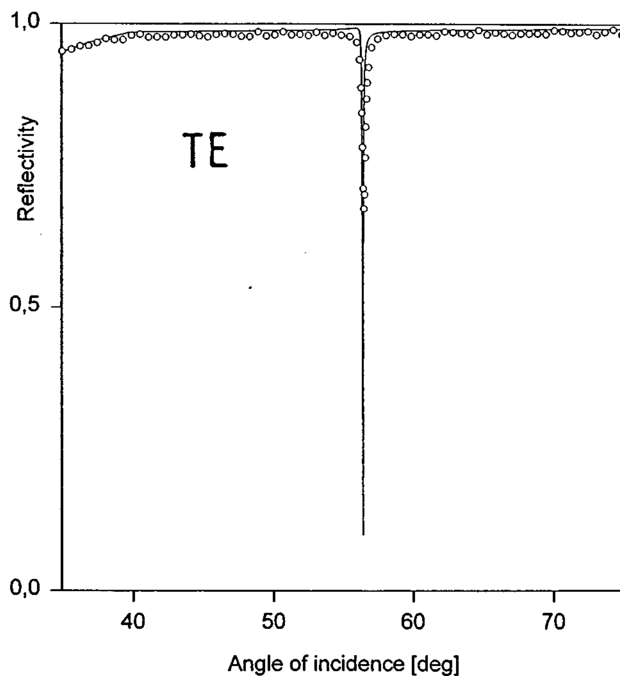

FIG. 7. TE and TM waveguide modes of a poled polymer (polymethacrylate with azobenzene side chains) with corresponding model fit used for retrieving the anisotropic refractive index and layer thickness.

The very same arrangement can be used to excite waveguide modes. The optical properties of the sample have to

match at least the cutoff conditions[3] given by the refractive indices of all media and the layer thickness. Waveguide modes exist in two forms: the so called TE modes (transversal electric) which are excited with s-polarized light and the TM modes (transversal magnetic) which need p-polarized light for excitation. If a sample is capable of guiding both type of modes the anisotropy of the sample can be determined without any ambiguity. Figure 7 shows the corresponding reflectivity scan of a poled polymer (polymethacrylate with azobenzene side chains) on a gold surface with a uniaxial arrangement of the polarizable units.

The described experimental platform can be further extended for other techniques by slight modifications. Examples would be dynamic and static light scattering as well as Brewster angle autocorrelation spectroscopy.[17]

ACKNOWLEDGMENTS

The authors thank Professor Möhwald for encouraging discussions and for providing financial support and also Dr. Martina Bree for helpful discussions and proofreading of the manuscript. R. Teppner thanks Professor Eichler for supervising his diploma thesis.

[1] R. M. Azzam and N. M. Bashara, *Ellipsometry and Polarized Light* (North Holland, Amsterdam, 1979).
[2] H. Raether, *Springer Tracts in Modern Physics*, Vol 111: *Surface Plasmons on Smooth and Rough Surfaces and on Gratings* (Springer, Berlin, 1988).
[3] R. G. Hunsperger, *Integrated Optics: Theory and Technology* (Springer, Berlin, 1991).
[4] P. S. Hauge, Surf. Sci. **96**, 108 (1980).
[5] F. L. MacCrackin, E. Passaglia, R. R. Stromberg, and H. L. Steinberg, J. Res. Natl. Bur. Stand. Sec. A **67**, 108 (1963).
[6] D. Beaglehole, Physica B & C **100**, 163 (1980).
[7] W. Knoll, *Materials Science & Technology*, Vol. 12, *Structures and Properties of Polymers* (Chemie, Weinheim, 1993).
[8] E. Kretschmann, Opt. Commun. **6**, 185 (1972).
[9] E. Burstein, W. P. Chen, Y. J. Chen, and A. Hartstein, J. Vac. Sci. Technol. **11**, 1004 (1974).
[10] D. Hönig and D. Möbius, J. Phys. Chem. **95**, 4590 (1991).
[11] S. Henon and J. Meunier, Rev. Sci. Instrum. **62**, 936 (1991).
[12] M. Lösche, E. Sackmann, and H. Möhwald, Ber. Bunsenges. Phys. Chem. **10**, 848 (1983).
[13] R. Reiter, H. Motschmann, H. Orendi, A. Nemetz, and W. Knoll, Langmuir **8**, 1784 (1992).
[14] E. Aust, W. Hickel, H. Knobloch, H. Orendi, and W. Knoll, Mol. Cryst. Liq. Cryst. **227**, 49 (1993).
[15] H. Riesenberg, *Handbook of Microscopy* (VEB Technik, Berlin, 1988).
[16] M. Harke, M. Stelzle, and H. Motschmann, Thin Solid Films **284**, 412 (1996).
[17] C. Lautz, J. Kildae, and Th. Fischer, J. Chem. Phys. **106**, 7448 (1997).